Chemical Physics Letters 751 (2020) 137535

Contents lists available at ScienceDirect

Chemical Physics Letters

journal homepage: www.elsevier.com/locate/cplett

Research paper

Laser patterning induced the tunability of nonlinear optical property in silver thin films

Zhengwang Li[a], Ruijin Hong[a,*], Qingyou Liu[b], Qi Wang[a], Chunxian Tao[a], Hui Lin[a], Dawei Zhang[a]

[a] Engineering Research Center of Optical Instrument and System, Ministry of Education and Shanghai Key Lab of Modern Optical System, University of Shanghai for Science and Technology, No. 516 Jungong Road, Shanghai 200093, China
[b] Key Laboratory of High-temperature and High-pressure Study of the Earth's Interior, Institute of Geochemistry, Chinese Academy of Sciences, Guiyang 550081, China

HIGHLIGHTS

- The surface of the patterned Ag thin films is covered by periodic microstructure.
- The volume fractions of Ag and Ag_2O are dependent on laser scanning rate.
- LSPR was observed in the as-irradiated samples.
- These samples exhibit tunable self-defocusing nonlinearity.

ARTICLE INFO

Keywords:
Laser patterning
Ag-Ag_2O composite films
Laser scanning rate
Optical properties
Charge transfer

ABSTRACT

Patterned Ag thin films were obtained through laser irradiation at ambient conditions. We investigated the effects of laser scanning rate for the structure and optical properties of patterned Ag films. XPS results show that the volume fractions of Ag and Ag_2O are dependent on the laser scanning rate. The localized surface plasmon resonance was observed in the as-irradiated samples and increased with the acceleration of the scanning rate. Moreover, with the variations of laser scanning rates and excitation energy, these samples exhibit tunable self-defocusing nonlinearity caused by charge transfer and the enhanced electromagnetic field at the interface between Ag and Ag_2O.

1. Introduction

Optical limiters show a reduced transmittance as a function of laser irradiation or flux and can be used to shelter the eyes and sensitive optics from laser harm. Numerous work has been done to develop perfect broadband optical limiting (OL) materials based on mechanisms like reverse saturable absorption [1], multiphoton absorption [2], and nonlinear scattering [3]. Noble metal nanomaterials like gold and silver have drawn considerable attention because of their unusual photoelectric properties as well as the potential applications in photon technology. Their linear optical properties are believed to be dominated by surface plasmon resonance (SPR), which also improves their nonlinear optical (NLO) response [4–6]. However, due to the interband transition and the fixed carrier density, the noble metals have a high optical loss, and their applications in integrated optics are limited [7,8]. To improve their optical properties, thin films based on metal and semiconductor materials have been proposed owing to their high degree of optical nonlinear and ultra-fast time response [9,10]. There are many methods to fabricate metal–semiconductor materials, such as chemical synthesis, chemical vapor deposition, doping, and so on. However, these methods involve chemical pollution and high cost.

Laser patterning is a technology that uses the heating effect of laser ablating the surface materials of metals to leave persistent patterns. The irradiated area will be oxidized at ambient conditions. Compared with the methods mentioned above, it has many advantages, such as flexibility, high quality, high speed, and no pollution [11–13]. For the patterned metal thin films, in which metals and oxides are tightly coupled to produce different functions, show properties far beyond individual structures. Generally, the NLO properties of metal–semiconductor films can be influenced by the energy transfer among the hybrids system, the SPR of noble metal nanoparticles, the plasmon-excition interaction, and the resultant local field environment [14]. Since the physical and optical properties of the hybrid system are profoundly affected by the size, shape and composition, strategies for the fabrication of metal–semiconductor hybrid materials become more attractive [15], and the accuracy and flexibility of laser patterning technology are reflected.

* Corresponding author.
E-mail address: rjhong@usst.edu.cn (R. Hong).

https://doi.org/10.1016/j.cplett.2020.137535
Received 5 April 2020; Received in revised form 24 April 2020; Accepted 24 April 2020
Available online 25 April 2020

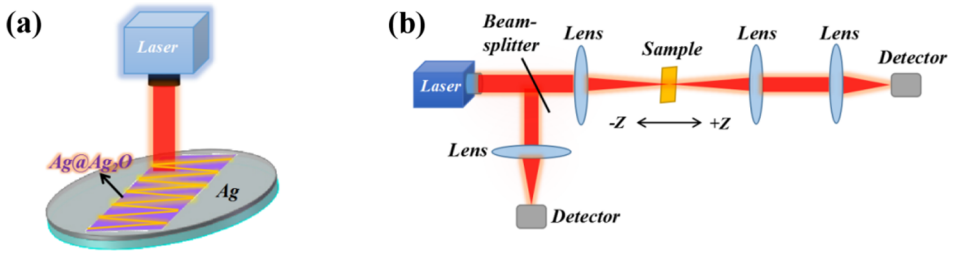

Fig. 1. (a) Schematic of the laser irradiation process, and (b) Z-scan system.

In this work, patterned silver thin films with periodic microstructures were obtained by laser irradiation. We explored the NLO properties of silver and patterned silver thin films at 1550 nm with a mode-locked picosecond laser. Moreover, the surface morphology, crystal structure, optical linearity, composition, and the electric field of the samples were investigated.

2. Experiment

The Ag thin film was deposited on the glass substrate by electron beam evaporation using a silver target (99.99%) at room temperature. The chamber was evacuated to a base pressure of less than 5×10^{-4} Pa, the working pressure was 0.8 Pa, and the deposition rate is about 2 nm/min. The layer was 100 nm monitored with the quartz crystal microbalance, denoted as S1. Then, it would be irradiated by Nd: YAG 1064 nm laser under ambient conditions with different scanning rates. The process of laser treatment was shown in Fig. 1(a). The laser was operated at 0.2 W; the pulse width was 100 ns, both the scanning line spacing and beam diameter were 0.01 mm. Besides, the scanning rate set as 2000, 2500, 3000, and 3500 mm/s, respectively. These as-irradiated thin films were denoted as S2-S5, respectively.

Z-scan is a single-beam experimental technique with high sensitivity, which is utilized for measuring the NLO properties of materials, as shown in Fig. 1(b). The mode-locked picosecond laser (Menlosystems, 100 MHz with a 2 ps pulse width) at 1550 nm with different incident intensities and the Gaussian beam is focused by 15 mm focal length lens. The surface of the samples was observed through the confocal microscopy and atomic force microscopy (AFM). The crystal structure and absorption spectra of the samples were obtained by X-ray diffraction (XRD) and dual beam spectrophotometer, respectively. The surface components of the samples were characterized by X-ray photoelectron spectroscopy (XPS). Furthermore, the Finite element method was employed to investigate the electric field of the as-deposited Ag thin film and patterned Ag thin films.

3. Results and discussion

3.1. Optical characterization

The confocal microscopy and AFM images of the samples are shown in Fig. 2. The as-deposited Ag thin film is continuous with a smooth surface. However, after laser patterning, the machined surfaces were covered with periodic microstructures at different scanning rates, which caused by the phase shift of laser spots along the scanning direction leading to the formation of grid-like surfaces [16]. Furthermore, Ag films highly tend to agglomeration by heating. In the case of laser irradiation, the laser energy is transferred to the Ag film, resulting in the melting of the film [17]. With the scanning rate increasing, the area of oxidized material in a specific area decreases, and the width (white part) between two adjacent elements increases. Specifically, in order to retain more Ag materials, a higher laser scanning rate is necessary to reduce the thermal effect of laser on the metal. The inserted AFM images in Fig. 2(b-e) and Fig. 2(a) are the surface morphologies of local areas of Ag thin films with and without laser irradiation, respectively. The gross morphology of the as-deposited Ag thin film is a smooth one. After modification by laser, the materials in the irradiated area were dissolved and then solidified to form spherical or ellipsoid, which means that good texture nanoparticles and a bumpy landscape can be obtained. The surface roughness values of the samples are 2.1, 10.2, 9.2, 9.8, and 8.7, respectively, as shown in Fig. 2(f). Compared to that of the as-deposited Ag film, the roughness value (RMS) of these as-irradiated samples increased significantly and reached around 9 nm.

XRD patterns of the as-deposited Ag and patterned Ag thin films are shown in Fig. 3(a). The as-deposited Ag thin film exhibits two diffraction peaks at around 38.12°(2θ) and 44.26°(2θ), corresponding to (1 1 1) and (2 0 0) plane of cubic Ag phase (JCPDS No. 89-3722), respectively. It is evident that the silver grains have a preferential orientation along the (1 1 1) crystal direction. In general, for non-epitaxial deposition, the film structure tends to be (1 1 1) or (0 0 1) planes due to the minimum surface free energy [18,19]. After modification by laser, peaks at around 38.14°(2θ) and 44.4°(2θ) correspond to (1 1 1) and (2 0 0) plane of Ag phase (JCPDS No. 89–3722), respectively. The further shift of the diffraction peaks indicates that the film stress increases. Besides, it should be noted that when the laser is applied to the surface of the Ag sample at a lower scanning rate, the thermal effect is more obvious and more silver is removed, resulting in the diffraction peak intensity being lower than that of the sample with a faster scanning rate. No prominent phase of oxides was observed in the as-irradiated samples due to its poor crystal quality.

The absorption spectra of the samples are shown in Fig. 3(b). Owing to the successive structure of as-deposited Ag thin film, no obvious absorption peak was observed [20]. However, these as-irradiated samples exhibited obvious LSPR peaks in the visible band and increased with the increase of scanning rate. Laser irradiation has a positive influence on LSPR phenomena, which can be explained through the existence of nano-ellipsoid structures of Ag thin films after laser irradiation [21], and the intensity of LSPR is related to the amount of silver treated. Moreover, in addition to the surface plasmon absorption of the as-irradiated samples, there are slight absorption bands in the UV wavelength region. These peaks correspond to the light absorption produced by the interband transition [22].

Fig. 4 reveals the representative XPS spectra of samples. Fig. 4(a) shows the Ag 3d doublets of S1 with binding energies at 374.4 eV and 368.4 eV assigning to Ag^0 $3d_{3/2}$ and Ag^0 $3d_{5/2}$, respectively [23]. After irradiating the Ag thin film at a lower scanning rate of 2000 mm/s, Ag 3d peaks can be fitted into four peaks, as shown in Fig. 4(b). Besides the peaks of Ag^0, the peaks situated at 374 eV and 368.1 eV were corresponding to Ag^+ [24], which demonstrates the formation of Ag_2O after laser irradiation. Moreover, the content of Ag^0 and Ag^+ on S2 is 23.1% and 76.9%, respectively. Observably, the Ag^+ content on S2 is greater than that of Ag^0, which indicates the surface of the Ag sample was mostly oxidized when irradiated at a low laser scanning rate. Fig. 4(c) shows the XPS spectrum of S5, the laser scanning rate is 3500 mm/s, which is higher than that of S2. The binding energies at 368.1, 368.4, 374, and 374.4 eV are ascribed to the signals of Ag^+ $3d_{5/2}$, Ag^0 $3d_{5/2}$, Ag^+ $3d_{3/2}$ and Ag^0 $3d_{3/2}$, respectively, which is similar to S2. However, the content of Ag^0 and Ag^+ on S5 changed, where the content of Ag^0 increased to 40.21% and Ag^+ decreased to 59.79%. To some extent, the

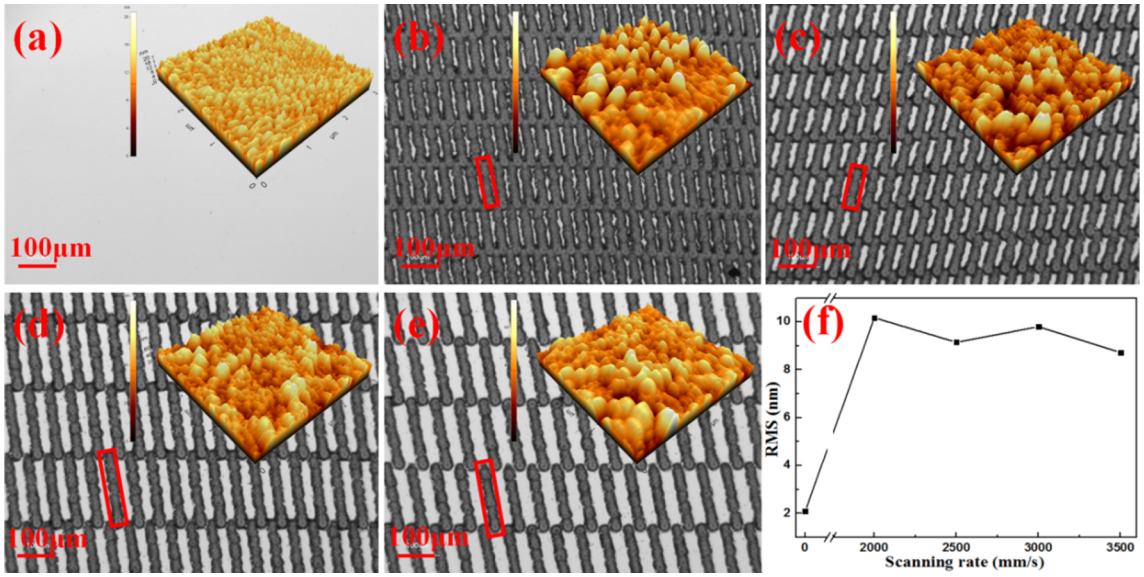

Fig. 2. (a-e) Confocal microscopy pictures and AFM images of samples with different laser scanning rates, and (f) the surface roughness of samples as a function of laser scanning rate.

acceleration of the laser scanning rate can reduce the thermal interaction time and the oxidation degree of Ag thin film. Fig. 4(d) exhibits the O 1 s spectra peaks of the samples, which can be divided into two peaks at 532.7 eV, and 531.4 eV, respectively. The former is ascribed to Ag-O bonding in Ag_2O structure, and the latter is hydroxylic [25,26], suggesting the presence of Ag_2O in the as-irradiated samples. The co-existence of Ag and Ag_2O in the as-irradiated samples is clearly proved by XPS results.

3.2. NLO properties

In a nonlinear regime, the total absorption coefficient α can be described as $\alpha(I) = \alpha_0 + \beta(I)I$, where α_0, $\beta(I)$, and I represent the linear absorption coefficient, the nonlinear absorption coefficient, and the laser intensity, respectively. The normalized transmittance $T_{Norm}(z)$ are fitted by the following equation:

$$T_{Norm}(z) = \frac{\ln[1 + q_0(z)]}{q_0(z)}$$

Here $q_0(z) = \beta(I_0 L_{eff})/(1 + z^2/z_0^2)$, $L_{eff} = [1 - e^{-\alpha_0 L}]/\alpha_0$, where I_0, L_{eff}, z, z_0, and L are the peak intensity at the beam-waist, the sample's effective path length, the straight-line distance between the sample and the focal point, the diffraction length of the beam and the thickness of the sample, respectively.

Fig. 5(a-c) shows the normalized transmittance of as-deposited Ag and patterned Ag thin films obtained through an open aperture Z-scan system with different input power densities, and the excitation wavelength is 1550 nm. When the peak irradiance incident on samples is 5.2×10^{-4} GW/cm^2, no distinct nonlinear absorption behavior was observed in S1. However, these patterned Ag samples show normalized transmittance valleys when they are close to the focus (high intensity), indicating the presence of reserve saturable absorption (RSA) in Ag-Ag_2O thin films. Moreover, the depth of the normalized transmittance valleys of these Ag-Ag_2O samples will deepen with the increase of laser scanning rate. When the peak irradiance energy increased to 9.8×10^{-4} GW/cm^2 and 3.1×10^{-3} GW/cm^2, respectively, as before, no obvious nonlinear absorption behavior was observed in S1. However, the valley depth of Ag-Ag_2O samples increases and the gap between the curves becomes larger, as shown in Fig. 5(b) and (c). The corresponding nonlinear optical coefficient β is shown in Fig. 5(d). At the same excitation energy, β shows positive and increases with the acceleration of laser scanning rate, which indicates the effect of laser irradiation on β enhancement and shows that the patterned Ag thin films have tunable optical nonlinearity. Moreover, when the excitation energy is different,

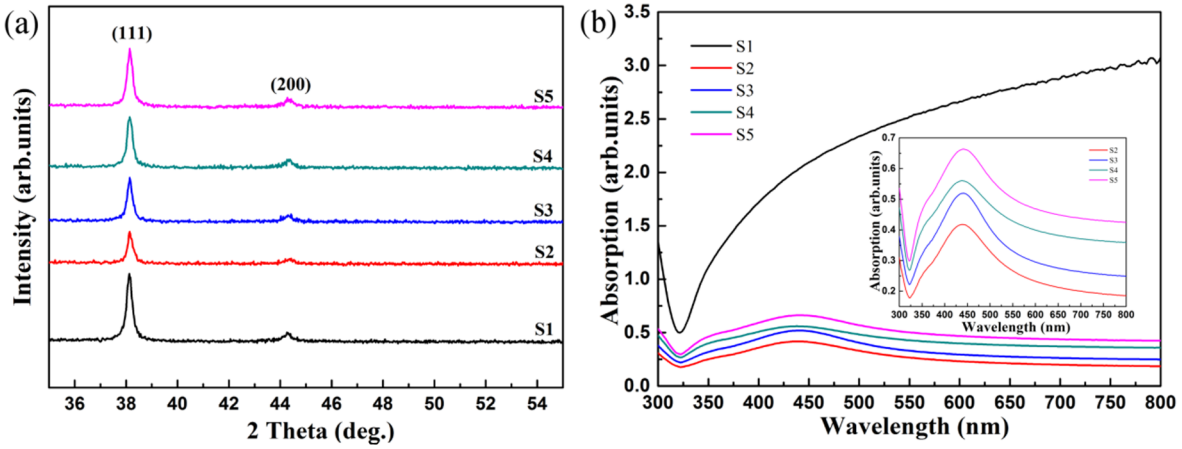

Fig. 3. (a) The XRD patterns and (b) Absorption spectra of samples before and after laser irradiation.

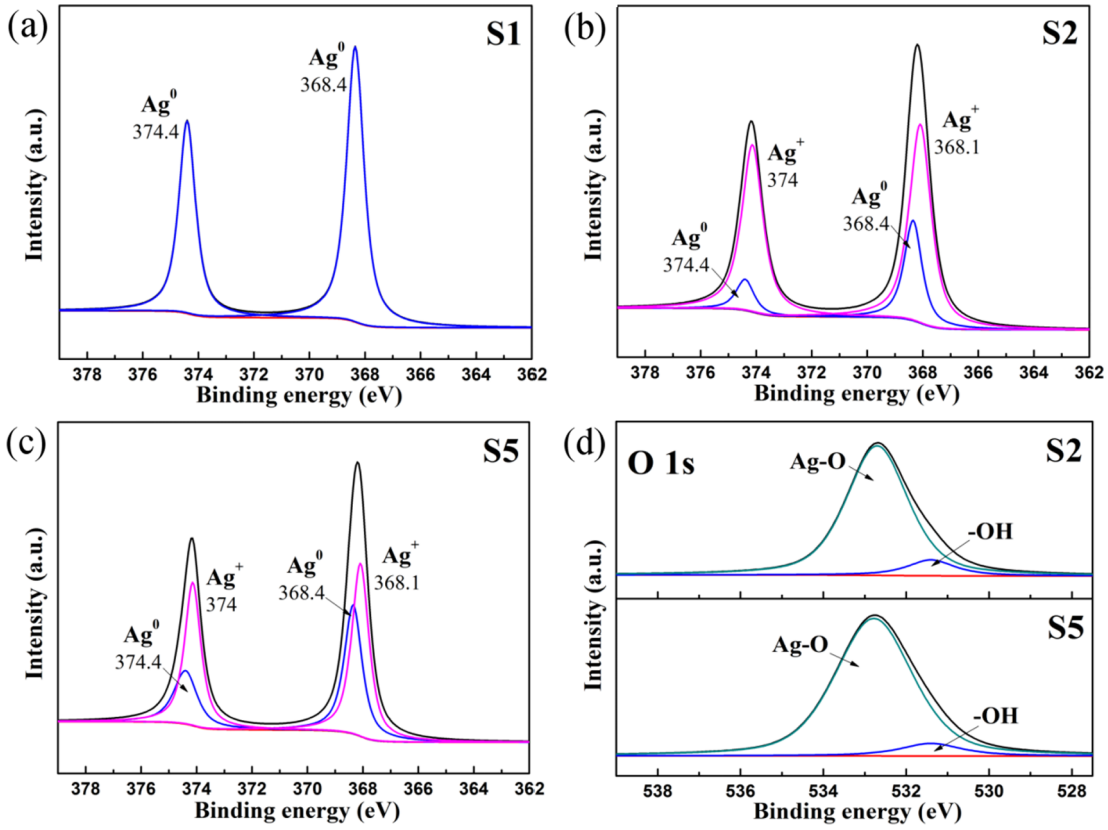

Fig. 4. XPS spectra of (a-c) Ag3d for S1, S2, S5, and (d) O1s for S2 and S5.

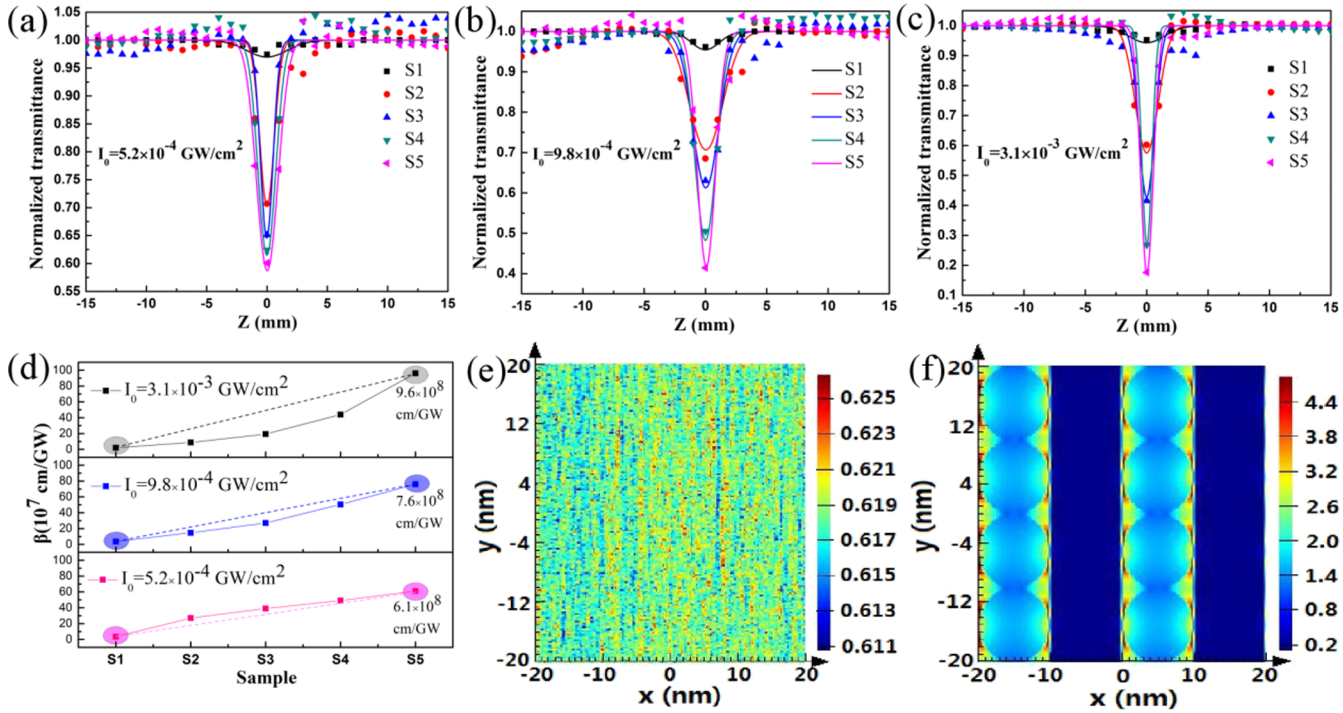

Fig. 5. (a-c) Open aperture Z-scan curves of the samples at different laser power densities; (d) the value of nonlinear absorption (β) of the samples; the FDTD simulated electric field amplitude patterns of samples (e) before and (f) after laser irradiation.

the change rate of β value among samples is also different. Under the excitation of 3.1 × 10^{-3} GW/cm^2, β has the maximum change rate from 2 × 10^7 cm/GW to 9.6 × 10^8 cm/GW.

The observed RSA performance is a clear signal of OL activity in materials, which is usually caused by nonlinear absorption, excited state absorption, and multiphoton absorption mechanism [27]. Generally, the RSA behavior of materials originates from the absorption process, which is determined by secondary photons bringing excited

electrons from the lower conduction band to the higher conduction band [28]. Besides, when the intensity of the incident laser is constant, the optical nonlinearity response of these patterned silver samples increases with the increase of the silver concentration, which is attributed to the increase of the molecular density and the high ionic mobility of the Ag ions affect the change of the electrical transport properties [29]. Concurrently, the enhanced electromagnetic field at the interface between Ag and Ag_2O will rapidly enhance RSA response [30]. In order to investigate the electromagnetic field of bare Ag and patterned Ag samples, the finite element method was applied. In this simulation, a 1550 nm laser is perpendicular to the x-y plane of the sample, and the polarization direction is along the y-axis. The simulated electric field of the samples is shown in Fig. 5(e-f). The maximum electric field strength of the samples with and without laser irradiation is 4.4 and 0.625, respectively. Obviously, the electric field strength of patterned Ag samples is stronger than that of bare Ag, which ensures that the nonlinear absorption effect of patterned Ag samples is more clear, as shown in Fig. 5(a-c). Therefore, the simulation results are consistent well with nonlinear absorption phenomena.

4. Conclusion

In this study, patterned Ag samples were obtained by laser irradiation with different scanning rates under ambient conditions. We investigated the influences of laser irradiation on the structure and optical properties of patterned Ag thin films. The results show that the surface of patterned Ag thin films is covered by periodic microstructure after laser irradiation, and the irradiated area varies from continuous film to nano-ellipsoid with corresponding the surface plasmon resonance in the visible region. XPS analysis shows that a different amount of Ag_2O will be formed when the as-deposited Ag films irradiated by laser at different scanning rates. The observed nonlinear absorption is explained by charge transfer and the enhanced electromagnetic field at the interface between Ag and Ag_2O, which is in accordance with the results of FDTD simulation.

CRediT authorship contribution statement

Zhengwang Li: Writing - original draft, Software. **Ruijin Hong:** Writing - review & editing, Supervision. **Qingyou Liu:** Investigation. **Qi Wang:** Data curation. **Chunxian Tao:** Data curation. **Hui Lin:** Formal analysis. **Dawei Zhang:** Project administration, Validation.

Declaration of Competing Interest

The authors declare that they have no known competing financial interests or personal relationships that could have appeared to influence the work reported in this paper.

Acknowledgement

This work was partially supported by the National Natural Science Foundation of China (61775140, 61775141), and the Shanghai foundation for Science and technology innovation action plan (1714220060).

References

[1] Y. Peng, G. Wang, C. Yuan, J. He, S. Ye, X. Luo, J. Alloy. Compd. 739 (2018) 345–352.
[2] J.L.T. Chen, V. Nalla, G. Kannaiyan, V. Mamidala, W. Ji, J.J. Vittal, New J. Chem. 38 (2014) 985–992.
[3] P. Chen, P. Wu, X. Sun, J. Lin, W. Ji, K. Tan, Phys. Rev. Lett. 82 (1999) 2548–2551.
[4] Y. Fang, J. Chem. Phys. 108 (1998) 4315–4318.
[5] G. Wang, Y. Zhang, Y. Cui, M. Duan, M. Liu, J. Phys. Chem. B 109 (2005) 1067–1071.
[6] P. Galletto, P.F. Brevet, H.H. Girault, R. Antoine, M. Broyer, J. Phys. Chem. B 103 (1999) 8706–8710.
[7] G.V. Naik, V.M. Shalaev, A. Boltasseva, Adv. Mater. 25 (2013) 3264–3294.
[8] Alberto Comin, Liberato Manna, Chem. Soc. Rev. 43 (2014) 3957–3975.
[9] M. Fu, K. Wang, H. Long, G. Yang, P. Lu, F. Hetsch, A.S. Susha, A.L. Rogach, Appl. Phys. Lett. 100 (2012) 63117–63119.
[10] F. Nan, S. Liang, X. Liu, X. Peng, Q. Wang, Appl. Phys. Lett. 102 (2013) 163112–163116.
[11] W. Jiang, X. Xie, X. Wei, W. Hu, Q. Ren, Z. Zou, Opt. Mater. Express 5 (2017) 1565–1574.
[12] M. Xin, Q. Jing, F. Yun, Adv. Mat. Res. 602 (2012) 929–933.
[13] K.S. Zelenskaab, S.E. Zelenskya, L.V. Poperenkoa, K. Kanevc, V. Mizeikisc, V.A. Gnatyukd, Opt. Laser Technol. 76 (2016) 96–100.
[14] G. Ma, S. Tang, J. He, Y. Yang, M. Nogami, Appl. Phys. Lett. 84 (2004) 4684–4686.
[15] U. Soni, P. Tripathy, S. Sapra, J. Phys. Chem. Lett. 5 (2014) 1909–1916.
[16] Q. Zhang, Q. Wang, Z. Zhang, H. Su, Y. Fu, J. Xu, Mat. Sci. Semicon. Proc. 107 (2020) 104864–104871.
[17] S.J. Henley, J.D. Carey, S.R.P. Silva, Phys. Rev. B 72 (2005) 195408.
[18] R. Hong, X. Wang, J. Ji, C. Tao, D. Zhang, Appl. Surf. Sci. 356 (2015) 701–706.
[19] I. Petrov, P.B. Barna, L. Hultman, J.E. Greene, J. Vac. Sci. Technol. A 21 (2003) S117–S128.
[20] S.A. Maier, Springer 52 (2007) 49–74.
[21] R. Hong, W. Shao, W. Sun, C. Deng, C. Tao, D. Zhang, Opt. Mater. 77 (2018) 198–203.
[22] B. Balamurugan, T. Maruyama, J. Appl. Phys. 102 (2007) 34306–34310.
[23] T. Potlog, D. Duca, M. Dobromir, Appl. Surf. Sci. 352 (2015) 33–37.
[24] M. Li, Y. Wang, Y. Xing, J. Zhong, Solid State Sci. 99 (2020) 106062–106067.
[25] F. Yu, Y. Chen, Y. Wang, C. Liu, W. Ma, Appl. Surf. Sci. 427 (2018) 753–762.
[26] H. Xu, J. Xie, W. Jia, G. Wu, Y. Cao, J. Colloid Interf. Sci. 516 (2018) 511–521.
[27] L. Polavarapu, N. Venkatram, W. Ji, Q. Xu, A.C.S. Appl, Mater. Inter. 1 (2009) 2298–2303.
[28] A. Sakthisabarimoorthi, S.A.M.B. Dhas, M. Jose, Mater. Chem. Phys. 212 (2018) 224–229.
[29] A. Sakthisabarimoorthi, S.A.M.B. Dhas, M. Jose, Mat. Sci. Semicon. Proc. 71 (2017) 69–75.
[30] G. Wang, Y. Zhang, Y. Cui, M. Duan, M. Liu, Opt. Commun. 249 (2005) 311–317.